Scripta Materialia 156 (2018) 51–54

Contents lists available at ScienceDirect

Scripta Materialia

journal homepage: www.elsevier.com/locate/scriptamat

Regular Article

Role of Cr-rich carbide precipitates in the intergranular oxidation of Ni-Cr alloys

Maria L. Sushko *, Daniel K. Schreiber, Kevin M. Rosso, Stephen M. Bruemmer

Pacific Northwest National Laboratory, 902 Battelle Boulevard, Richland, WA 99354, United States

ARTICLE INFO

Article history:
Received 31 May 2018
Received in revised form 10 July 2018
Accepted 10 July 2018
Available online xxxx

Keywords:
Corrosion
Oxidation
Alloy
Atom probe tomography
First-principle calculation

ABSTRACT

The influence of grain boundary Cr carbides on the intergranular oxidation behavior of a Ni-16Cr alloy is considered using atomistic-to-mesoscale model and atom probe tomography. Cr carbide strongly perturbs the collective reactive dynamics of oxidizing species and alloy elements in the intergranular region. Strong attractive interactions between oxygen and carbide create a driving force for Cr and Ni accumulation in the grain boundary adjacent to the carbide, and for the depletion of Cr and Ni ahead of the oxidation front beyond the carbide. The results shed light on the mechanism of carbide-assisted protection of the alloy against grain boundary corrosion/oxidation.

Grain boundary precipitates play a critical role in the susceptibility of materials to degradation and failure in aggressive environments. This is particularly evident when stress and environment combine to cause intergranular stress corrosion cracking (IGSCC) in high-temperature water environments. While the precise mechanism that controls IGSCC for Ni-base alloys in hydrogenated water is still debated [1–4], empirical studies have identified specific materials and thermo-mechanical histories that are linked to enhanced or degraded IGSCC resistance. These linkages include improved IGSCC resistance and a higher density of grain boundary Cr carbides in Ni-Cr and Fe-Cr alloys [5–7], for which two hypotheses have been put forward. In one, grain boundary Cr carbides impede IGSCC propagation through mechanical means [6,8]. Alternatively, it has been suggested that the precipitates alter the IG corrosion/oxidation behavior [6,9,10]. For example, the Cr-rich carbide favors the formation of Cr-rich IG oxides (e.g. Cr_2O_3) that are more protective than other commonly observed phases (e.g., MO-phase mixed oxides) [11]. It has also been observed that IG carbides impede grain boundary migration, which may further slow oxide growth that can rely on diffusion-induced grain boundary migration (DIGM) [10].

In this work, we build upon a novel atomistic-to-mesoscale model of IG oxidation [12] to consider the effect of a Cr-rich grain boundary precipitate (Cr carbide) on the oxidation behavior of a simulated Ni-16Cr alloy. The model treats the oxidation process using steady-state reactive dynamics, in which alloy elements and oxidizing species, driven by the gradient in chemical potentials, react in the grain boundary region. Chemical potentials are calculated using a parameter-free approach that couples elementary diffusion processes and mesoscale correlated fluctuation dynamics. The barriers for elementary diffusion of Ni and Cr species in the alloy, oxide and carbide phases are calculated using plane-wave density functional theory (DFT) and then used within classical DFT/Poisson-Nernst-Planck formalism for many-body correlated reactive dynamics. The total chemical potential of the system includes the Coulomb electrostatic, many-body electrostatic correlation, excluded volume and chemical short-range, e.g. energy cost for elementary diffusive hops or energy gain in oxide formation, components. Previously, the model was used in a semi-one-dimensional representation of the grain boundary consisting of the IG oxide region and the grain boundary region ahead. Simulations of the IG oxidation process for Ni-5Cr and Ni-4Al alloys predicted the formation of continuous porous oxides and porous oxide clusters, respectively, due to different relative diffusivities of matrix and alloying elements [12]. Here the semi-one-dimensional model is extended to a three-dimensional to include the alloy and an IG Cr carbide precipitate to study the role of the carbide on IG oxidation processes. The model output is directly compared with three-dimensional atom probe tomography (APT) observations of IG corrosion/oxidation around a Cr carbide particle at the nanoscale in a commercial Ni-16Cr alloy (alloy 600, Ni-16Cr-8Fe [at.%] plus minor elements) exposed to 338 °C, hydrogenated high-purity water under Ni-metal stable electrochemical conditions.

An APT reconstruction of the corroded grain boundary intersecting an IG Cr carbide precipitate is shown in Fig. 1. The same dataset is viewed with the grain boundary in cross-section (panel A) and plan view (panel B). Ions of Cr (metal, orange) and CrO (oxide, blue) are displayed in combination with isoconcentration surfaces at 6.5 at.% Cr (gray – outlining Cr depleted zones) and 50 at.% Cr + C (maroon –

* Corresponding author.
E-mail address: maria.sushko@pnnl.gov (M.L. Sushko).

https://doi.org/10.1016/j.scriptamat.2018.07.016
1359-6462/

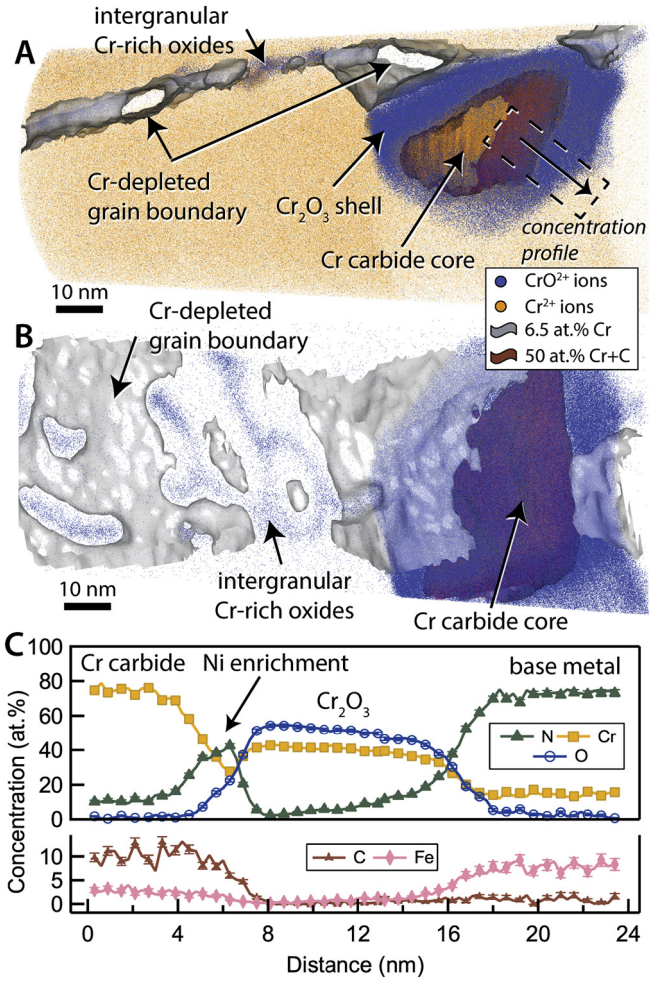

Fig. 1. APT characterization of intergranular oxidation in alloy 600 upon exposure to high-temperature hydrogenated water. 3D APT reconstruction viewed in the (A) cross-section and (B) plan view orientations depicting Cr-rich oxide and Cr-poor metal along the grain boundary and a partially oxidized intergranular Cr carbide. (C) Corresponding APT 1D concentration profile reveals a surprising Ni enrichment at the oxide/carbide interface. Error bars indicate 1σ from standard counting error.

outlining the Cr carbide). The IG oxide consists of narrow penetrations of Cr-rich oxide (blue dots) along the grain boundary plane. These oxides are surrounded by localized grain boundary depletion of Cr (gray surface). The IG oxide then intercepts the Cr carbide, depicted by the maroon surface. A thick Cr_2O_3 shell envelopes the Cr carbide core, and severe local depletion of Cr can be seen at the periphery of the particle near the grain boundary plane. We note that this material was not sensitized by thermal treatment and the observed intergranular Cr depletion is from Cr-rich oxide formation during corrosion and not from carbide precipitation. The interface between the carbide (left) and oxide (right) is further interrogated quantitatively using a 1D concentration profile in Fig. 1C. Both the carbide and oxide phases are Cr-rich. The oxide composition is consistent with Cr_2O_3 and the carbide is likely either M_7C_3 or $M_{23}C_6$, although the APT data alone cannot make definitive phase identifications. Clear segregation of Ni to the Cr_2O_3/carbide interface can be seen, increasing to ~45 at.% Ni from ~10 at.% in the carbide and <1 at.% in Cr_2O_3. Similar segregation was observed at the oxide/carbide interface for all crystallographic faces of the Cr carbide. Additional APT analyses of IG carbides oxidized in hydrogenated water at the Ni/NiO stability (rather than the Ni-metal stable condition used here) have identified similar Ni segregation to the carbide/oxide interface [13]. Together these observations suggest that local Ni enrichment may be a key detail for understanding the role of grain boundary Cr carbide precipitates on the IG corrosion/oxidation behavior of these Ni-Cr alloys in high-temperature hydrogenated water, and their consequent effect on IGSCC.

The underlying mechanism of IG oxidation in the presence of a Cr carbide was revealed through atomistic-to-mesoscale simulations. The model schematically depicted in Fig. 2A consists of three regions: Ni-16Cr alloy, Cr carbide with $Cr_{23}C_6$ stoichiometry at one side of the grain boundary, and the grain boundary region itself. Within the model, the reactive transport of Ni, Cr and O was considered under constant flow conditions (see Methods for details) and the resulting distribution of species and their chemical potentials were analyzed. Simulations reveal a strong effect from the carbide on IG oxidation. The carbide, which can be viewed as a Cr-rich phase within the alloy with 16% Cr content, changes the local Cr chemical potential that manifests significant changes in the local oxidation process and the distribution of species nearby.

For example, the simulations predict Ni depletion at the oxidation front in close vicinity to the carbide, which is not observed in the absence of a carbide (Fig. 2B,D). Ni depletion adjacent to the carbide is local, only 0.3 nm wide. Cr is also partially depleted from the grain boundary region at the oxidation front in the presence of a carbide. However, in contrast to the Ni distribution, a low concentration of Cr is observed in the grain boundary region (Fig. 2C). Furthermore, the Cr distribution at the grain boundary behind the oxidation front points to continuous oxidation and to the formation of porous Cr_2O_3 oxide in the absence of the carbide (Fig. 3A), consistent with our previous simulations and experimental observations for Ni-5Cr alloys [12,14]. Introducing a carbide region at one side of the boundary hinders oxide formation (Fig. 3A). The concentration of oxidized Cr becomes, on average, ten times smaller than that without a carbide, marking the formation of a less dense oxide phase (Fig. 3A).

The analysis of the excess chemical potential of Ni, Cr and O sheds further light onto the underlying driving forces responsible for the observed oxidation behavior (Fig. 3B–D). In the absence of a carbide the chemical potentials for Ni and Cr in the grain boundary region are oscillatory, with Cr having a much stronger driving force to react with oxygen and form the oxide (Fig. 3B). The excess chemical potential of oxygen at the grain boundary also has an oscillatory character with the same periodicity as that for Cr This observation is in-line with our previous simulations and experimental data for Ni-5Cr alloy [12]. Oscillations in the chemical potential reflect the interactions of Ni and Cr with their corresponding atomic sites. While the Cr chemical potential is fully symmetric in the alloy region ahead of the oxidation front, an asymmetric chemical potential profile is observed across the oxidized grain boundary (Fig. 3B and Fig. S1 in Supporting Information). These differences in the oscillation amplitude reflect differences in the structure of alloy/oxide interface and the structure of the porous Cr_2O_3 oxide, favoring preferential diffusion of Cr from one side of the grain boundary in each (y,z) plane (Fig. 3A). Depending on the structure of the interface, either one side or the other can be a preferential source of Cr ions, resulting in the observed asymmetry of the chemical potential curves (see Fig. S1 in Supporting Information). Structurally, this effect can manifest as an asymmetry in the depth of Cr depletion on the sides of grain boundary around the oxide, as observed both in experimental [11] and calculated (Fig. 3A) Cr redistributions.

The presence of a carbide on one side of the grain boundary significantly changes the chemical potential of the species by further breaking the symmetry across the grain boundary (Fig. 3C–D). For Ni and Cr, the driving force favors their accumulation at oxide/metal interface. In contrast, oxygen is driven towards the carbide interface (Fig. 3D). These opposing effects hinder oxidation near the carbide, as evidenced by the lower density of Cr reacted with O within the oxide region for the with carbide case of Fig. 3A. Moreover, strong driving forces for Ni and Cr accumulation at the grain boundary side opposite to the carbide region (i.e. oxide/metal interface) lead to partial depletion of Cr and Ni ahead of the oxidation front (Fig. 3C–D), further impeding IG oxidation. With regards to mechanistic hypotheses put forward in prior work, our